Solar Radiative Heating in the Presence of Aerosols

Abstract: A theoretical study is carried out to evaluate the effects of aerosols on the shortwave flux divergence in the lower troposphere (0-2 km) by using four computational methods: Gauss-Seidel iteration, a reference method by which all orders of scattering are accounted for, and three approximations, primary scattering, no-scattering and median wavelength. By using these procedures, the radiative transfer equation is solved for a cloudless plane parallel atmosphere of infinite extent in the horizontal, but of finite extent in the vertical. The Gauss-Seidel procedure is taken as a standard and comparisons of the flux divergence are made by using various combinations of solar zenith angle, aerosol size frequency distribution and aerosol refractive index. In many of the simulations the median wavelength approximation gives accuracies comparable to those of the no-scattering approximation, in which case the choice of method is based on the required computational time. However, inaccuracies appear with all the approximations and the degree of superiority of one method over another depends on the aerosol and gaseous constituents of the model atmosphere.

Introduction

Recent observations of the flux divergence of short wave radiation (0.30-2.4 μ m) indicate that aerosols play a larger role in the absorption of solar energy than was previously suspected [1, 2]. In an attempt to quantify the impact of this additional absorption on global climate, various simulation calculations making use of terrestrial radiative transfer theories have been carried out [3-5]. The results of these studies indicate that an increase in the tropospheric aerosol concentration could lead to either a warming or a cooling of the atmosphere near the earth's surface.

Observational evidence that aerosol concentrations over large urban areas have increased due to man's activity has also been presented. The local climate in many of these large urban areas has been altered as a result of the presence of these anthropogenic aerosols. One atmospheric parameter that has been affected is the short wave flux divergence incident at the ground within cities [6–9].

In addition, a number of theoretical investigations have been carried out to determine the potential impact of these anthropogenic aerosols on the short wave radiative heat balance in the lower troposphere (approximately 0–2 km) [10, 11], commonly referred to as the atmospheric boundary layer.

In these various simulation studies, the equation of radiative transfer was solved by using various approximations. The method of approximation chosen is usually determined by weighing the computational time savings against the accuracy desired. Accurate modeling of radiative transfer in the presence of aerosols can go a long way in aiding experimental design of observational studies. In addition, precise simulation of multiple scattering and absorption by aerosols can aid in evaluating the sensitivity of flux divergence to changes in particular aerosol characteristics (e.g., size distribution and refractive index).

In the context of this paper, a solution of the transfer equation for short wave radiation will be considered a reference solution if it takes into account multiple scattering, and if its accuracy is the highest consistent with the available computational methods. The method chosen for the reference case is the iterative method of Braslau and Dave [12]. Extensive calculations based on this method are then used in evaluating the accuracy of three approximation methods that are much less demanding of computational time than the reference method. The three methods discussed in this paper are: (a) the *primary scattering approximation*, (b) the *no-scattering approximation*, and (c) the *median wavelength approximation*.

Calculation of radiative flux divergence

Assumptions and procedures

The model atmosphere we choose is assumed to be cloudless, plane parallel and horizontally homogeneous, but in-

Copyright 1978 by International Business Machines Corporation. Copying is permitted without payment of royalty provided that (1) each reproduction is done without alteration and (2) the *Journal* reference and IBM copyright notice are included on the first page. The title and abstract may be used without further permission in computer-based and other information-service systems. Permission to *republish* other excerpts should be obtained from the Editor.

homogeneous in the vertical direction. At the bottom of the atmosphere there is an idealized ground having the property that all radiation incident upon it is totally absorbed. Unfortunately the added computational burden necessary for considering the effects of ground reflection would have exceeded the time available for this effort. The solar spectrum from 0.3025 to 2.45 μ m is divided into 80 unequal intervals, and within each, the optical parameters of the atmospheric gases and aerosols are taken to be constant. The scalar form of the transfer equation is used, thereby neglecting polarization effects in the atmosphere. The aerosols are assumed to be spherical in shape and composed of a homogeneous material whose refractive index is independent of wavelength. Changes in the anthropogenic aerosols are assumed to take place within the bottom 200 mb (2 pascals) (0-2 km) of the atmosphere, the layer we have termed the radiation boundary layer. Finally, it is assumed that the downward radiation incident on the top of the radiation boundary layer is independent of the properties of the layer itself. This last approximation is based on the fact that the component of the upward flux at the top of the turbid layer which is backscattered by the underlying atmosphere is only a small fraction of the total incident flux, and therefore of minor significance. Under these arguments, the fluxes of direct solar radiation and the azimuth-independent component of the diffuse sky radiation incident at the top of the radiation boundary layer are obtained at 2° intervals in each of the 80 wavelength ranges through a spectral range from 0.3025 μ m to 2.45 μ m for each of four solar zenith angles of the model C atmosphere of Braslau and Dave [12]. These quantities are then used as input to carry out transfer calculations within the radiation boundary layer. The upward and downward quasi-monochromatic diffuse fluxes are evaluated at 20 equally spaced pressure levels within the 2-km-thick radiation boundary layer. From these results, the spectrally integrated upward and downward fluxes at these levels are computed. These data are then used to obtain the vertical profile of the flux divergence for each model considered.

• Equation of transfer for nonhomogeneous atmosphere The equation of transfer of a monochromatic beam of radiation of intensity $I(\tau; \mu, \phi)$ propagated at zenith angle θ = $\cos^{-1}\mu$ and azimuth ϕ through a plane-parallel, horizontally homogeneous atmosphere of normal optical thickness τ can be represented by the expression

$$\mu - \frac{dI(\tau; \mu, \phi)}{d\tau} = I(\tau; \mu, \phi) - \omega(\tau)J(\tau; \mu, \phi). \tag{1}$$

The source function is given by $J(\tau; \mu, \phi)$ and $\omega(\tau)$ is the albedo of single scattering of the particles.

The boundary conditions for Eq. (1) are given by

$$I(0; -\mu, \phi) = 0 I(\tau_a; \mu, \phi) = 0$$
(2)

where τ_a is the total optical depth for the atmosphere. We use the convention that $-\mu$ and μ are for the downward and upward directions, respectively. It is assumed that the atmosphere is illuminated by parallel solar radiation propagated in the $-\mu_0$, ϕ_0 direction with a net flux of $F(-\mu_0, \phi_0) = 1$ per unit area normal to its direction of propagation.

The method used for solving Eq. (1) is that given by Braslau and Dave [12]. It is presented here for completeness and to ensure continuity when discussing the solution to Eq. (1) in the radiation boundary layer.

The total optical thickness of the layer in question is due to Rayleigh scattering by gaseous molecules $\tau^{(s,r)}$, Mie scattering by aerosols $\tau^{(s,m)}$, absorption by gases $\tau^{(a)}$, and absorption by aerosols $\tau^{(a,m)}$. Thus we can write

$$\tau = \tau^{(s,r)} + \tau^{(s,m)} + \tau^{(a,m)} + \tau^{(a)}. \tag{3}$$

The albedo of single scattering is given by

$$\omega(\tau) = \frac{\Delta \tau^{(s,m)} + \Delta \tau^{(s,r)}}{\Delta \tau} , \qquad (4)$$

where $\Delta \tau$ is determined from Eq. (3). The details of the method for computing the values of these quantities are given in [12].

The source function $J(\tau; \mu, \phi)$ is defined as

$$J(\tau; \mu, \phi) = \frac{1}{4} F \exp(-\tau/\mu_0) P(\tau; \mu, \phi; -\mu_0, \phi_0)$$

$$+\frac{1}{4\pi}\int_{-1}^{+1}\int_{0}^{2\pi}P(\tau;\mu,\phi;\mu',\phi')I(\tau;\mu',\phi')d\mu'\;d\phi', (5)$$

where F is the solar flux in the $(-\mu_0; \phi_0)$ direction. The function $P(\tau; \mu, \phi; \mu', \phi')$ is the normalized scattering phase function representing the distribution of the scattered radiation by a unit volume, which is being illuminated by a beam of unit strength from the direction μ', ϕ' and scattered in a direction μ, ϕ . For a unit volume consisting of both molecules and aerosols, this normalized phase function has the form

$$P(\tau; \mu, \phi; \mu', \phi') = T(\tau) M(\mu, \phi; \mu', \phi') + [1 - T(\tau)] R(\mu, \phi; \mu', \phi'),$$
(6)

where $T(\tau)$, the turbidity factor, is given by

$$T(\tau) = \frac{\Delta \tau^{(s,m)}}{\Delta \tau^{(s,m)} + \Delta \tau^{(s,r)}} . \tag{7}$$

The quantities $M(\mu, \phi; \mu', \phi')$ and $R(\mu, \phi; \mu', \phi')$ in Eq. (6) are the normalized Mie and Rayleigh scattering phase functions, respectively.

123

Several authors [12–15] have shown the utility of expanding the phase function in a Fourier series whose argument is the difference between the azimuth angles of the incident and scattered radiations. Furthermore, the intensity and source function can also be expanded in a Fourier series. Such an expansion permits the integration over azimuth to be achieved analytically. Since we are interested in flux, only the first term of the Fourier expansion need be evaluated. The upward and downward diffuse fluxes at a level τ are given by

$$F_{\rm u}(\tau) = 2\pi \int_0^1 I^{(1)}(\tau; \, \mu) \, \mu \, d\mu, \tag{8}$$

and

$$F_{\rm d}(\tau) = 2\pi \int_0^1 I^{(1)}(\tau; -\mu) \,\mu \,d\mu, \tag{9}$$

where $I^{(1)}(\tau; \mu)$ is the first term of the Fourier expansion written as

$$I(\tau; \mu, \phi) = \sum_{n=1}^{N} I^{(n)}(\tau; \mu) \cos((n-1))(\phi_0 - \phi).$$
 (10)

By substituting Eq. (10) and a similar expression for $J(\tau; \mu, \phi)$ into Eq. (1) and integrating over the azimuth angle, the basic transfer equation for the radiation boundary layer becomes

$$\mu \frac{dI^{(1)}(\tau_{b}; \mu, -\mu_{0})}{d\tau} = I^{(1)}(\tau_{b}; -\mu_{0}) - \omega(\tau_{b}) J^{(1)}(\tau_{b}; \mu, -\mu_{0}), \tag{11}$$

where τ_b is the optical depth within the radiative boundary layer at some height h. The boundary conditions for Eq. (11) are

$$I^{(1)}(\tau_{\text{Tb}}; -\mu) = 0$$
 (12)

and

$$I^{(1)}(\tau_{\rm Bb};\mu) = 0,$$
 (13)

where the quantities $\tau_{\rm Bb}$ and $\tau_{\rm Tb}$ are the normal optical depths at the bottom and top of the radiation boundary layer, respectively.

The source function $J^{(1)}(\tau_{\rm b}; \mu, -\mu_{\rm o})$ is given by

$$J^{(1)}(\tau_{\rm b}; \mu, -\mu_{\rm o}) = \frac{1}{4} I_{\rm o} \exp{(-\tau_{\rm Tb}/\mu_{\rm o})} \exp{[-(\tau_{\rm b} - \tau_{\rm Tb})/\mu_{\rm o}]}$$

$$\times P(\tau_{\rm b}; \mu, \mu_{\rm 0}) + \frac{1}{2} \int_{\rm 0}^{1} P(\tau_{\rm b}; \mu, -\mu_{\rm 1})$$

$$imes I^{(1)}(au_{
m Tb}; \, -\mu_1; \, \mu_0) \, \exp \left[-(au_{eta} - \, au_{
m Tb})/\mu_1
ight] \, d\mu_1$$

$$+ \frac{1}{2} \int_{-1}^{+1} P(\tau_{b}; \mu; \mu') I(\tau_{b}; \mu', -\mu_{0}) d\mu', \qquad (14)$$

where μ_1 is the cosine of the angle that the diffuse radiation incident on the top of the radiation boundary layer makes with respect to the local zenith. The quantity μ' is the cosine of the angle that the scattered radiation makes

with respect to the local zenith and I_0 is the intensity incident on top of the radiation boundary layer. Again the terms in Eq. (14) are azimuth independent.

The first term in Eq. (14) represents the contribution due to scattering of the direct short wave radiation on the top of the radiation boundary layer. The second term denotes the contribution due to the downward directed diffuse radiation incident on the top of the radiation boundary layer that originated from all directions (μ_1) in the upper hemisphere. Finally, the third term represents the contribution due to scattering in the radiation boundary layer itself.

• Basic model

The radiation boundary layer model is taken to extend through the lower 2 km of the atmosphere. The variations of pressure, temperature, water vapor, carbon dioxide, oxygen and ozone with height are those found between the surface and 2 km of model C of Braslau and Dave [12]. The total unscaled water vapor and ozone amounts are 1.826 gm/cm² and 0.005 cm-atm., respectively. To simulate aerosol contributions in the radiation boundary layer, the total number of particles in a unit column between the surface and 2 km in the model C was increased from 1.646×10^7 to 1.886×10^8 . The aerosol concentration was assumed to be uniform with height, and to have a value of 1.013×10^3 cm⁻³.

The refractive index (η) for anthropogenic aerosols is not well established. The aerosol observations of Cartwright et al. [16] over Sheffield, England taken some 20 years ago indicated that those aerosols were composed largely of carbonaceous material. Presumably, the major sources producing these aerosols were coal-burning sources. Present-day sources burn fuels containing less carbonaceous material; however, recent renewed interest in burning potentially large amounts of coal in place of oil led us to choose a carbonaceous aerosol for our calculations. By using the results of Twitty and Weinman [17] for carbonaceous aerosols, the upper limit for the model aerosol's refractive index was taken as 1.80-0.5 i. Aerosols made of such material are very strong absorbers and scatterers of short wave radiation. The lower limit is a nonabsorbing aerosol with $\eta = 1.50-0.0 i$.

The final parameter required for the computations is the size-frequency distribution of aerosol particles. Computations were made for two different distributions—the Junge distribution [18] and the Haze L distribution of Deirmendjian [19]. The Junge distribution is given by the relation

$$n(r) = c_1 r^{-(\beta+1)}, (15)$$

where n(r) is the number of particles per unit volume in a unit interval of radius centered at r, c_1 is the particle concentration at $r = 1 \mu m$, and β is a parameter de-

termined by the size spectrum of the particles. The distribution function for Haze L is written as

$$n(r) = ar^{\alpha} \exp\left(-br^{\gamma}\right),\tag{16}$$

where a, α , b, and γ are parameters which can be varied to fit the properties of a given aerosol. DeLuisi et al. [20] were moderately successful in fitting this relation to actual observations.

Values of the parameters of the two distributions that were used for these computations are: $a=4.9757\times 10^6$ cm⁻³ μ m⁻¹, b=15.1186, $\gamma=0.50$, $\alpha=2.0$, $c_1=8.83$ cm⁻³ μ m, and $\beta=3$. Data for c_1 and β were obtained from observations summarized by McClatchey et al. [21], while those for the Haze L model are from Deirmendjian [19].

The mass loading of particulate matter has been arbitrarily assumed to be the same for the two distribution functions. This required increasing the total number of particles in a unit vertical column from 1.886×10^8 for the Haze L function to 1.368×10^9 for the Junge distribution. Figure 1 shows a comparison of these two size distribution functions. The Junge distribution has a cutoff at particle radius $0.025~\mu m$ and an upper limit value for n(r) of $10~\mu m$.

In order to treat the attenuation of direct solar radiation due to atmospheric gases, the solar spectrum between 0.3025 and 2.45 μ m is divided into 80 unequal intervals. The absorption parameters for ozone, water vapor, carbon dioxide and oxygen were determined by plotting high resolution absorption data as a function of wavelength and then determining mean values of the absorption data for each of the 80 spectral bands. The spectral distribution of the absorption parameters are given by Braslau and Dave [12]. By the use of this distribution the attenuation of the radiation incident on the nth atmospheric level is evaluated from the expression

$$\exp\left[-\tau_n^{(a)}/\mu_0\right] = T_{wn}(\mu_0)T_{xn}(\mu_0)T_{cn}(\mu_0)T_{on}(\mu_0). \tag{17}$$

The transmission factors $T_{\rm wn}$, $T_{\rm xn}$, $T_{\rm cn}$, and $T_{\rm on}$ are for water vapor, oxygen, carbon dioxide, and ozone, respectively. The gaseous absorption undergone by the scattered radiation as it passes through the *n*th layer is computed from the equation

$$\exp\left[-\Delta \tau_n^{(n)}/\mu_0\right] = T_{i,n+1}(\mu_0)/T_{i,n}(\mu_0),\tag{18}$$

where $T_{i,n}$ is the transmission factor due to the *i*th gas at the *n*th level. The total optical thickness for all gases is obtained by summing the values for individual gases for each spectral region.

While the water vapor and carbon dioxide absorption can change considerably (due to line structure) within an absorption spectral interval, the 80 bands were chosen to minimize these variations. The overall accuracy of the approach is likely to be good provided the transmission remains fairly large (90 percent). Most of the absorption by

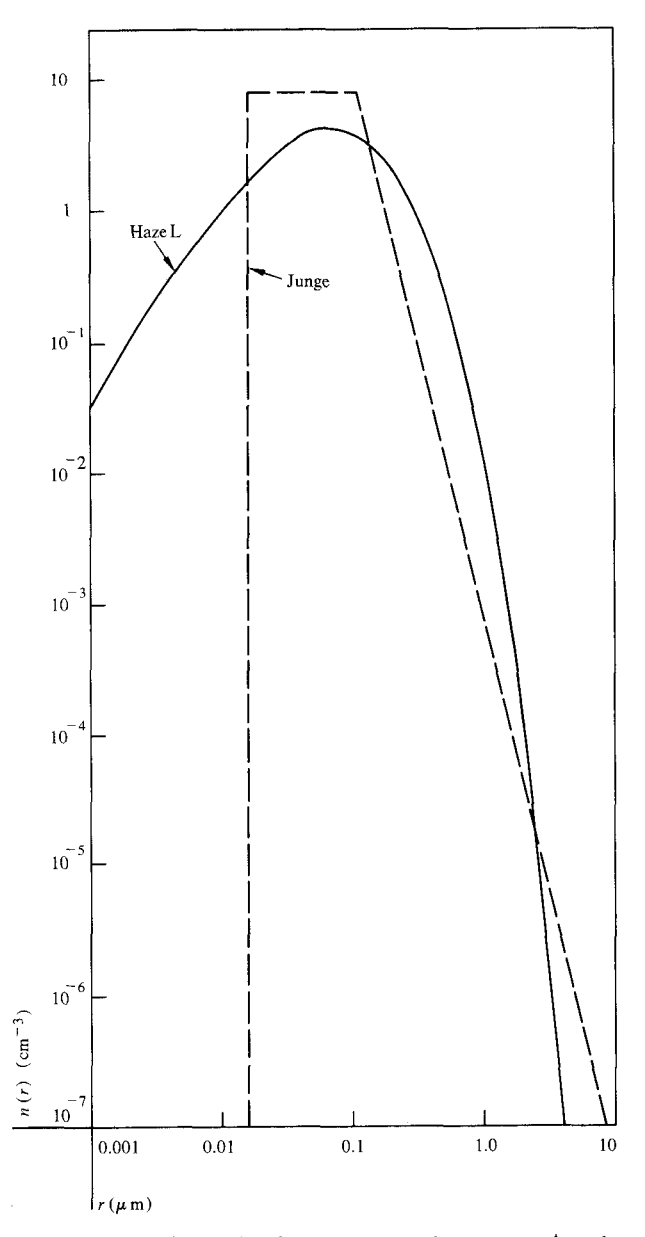


Figure 1 Size distribution for Haze L and Junge aerosol models, where n(r) is the density of particles in a sampling sphere of radius 1 μ m, centered at r.

the gases considered takes place in the troposphere. Here the fraction of energy in the spectral regions of strong absorption is about 15 percent of the total, and errors would modify the flux divergence only slightly. The largest error in determining gaseous absorption is in estimating the optical thickness when both scattering and absorption are present. As most of the scattering is in the forward direction for the bands considered, the solar-angle dependent formulation should be adequate. However, for very low zenith angles (when the diffuse beam is strong) errors

will arise from the μ_0 dependence. Bounds on these errors have been presented by Braslau and Dave [12].

• Multiple scattering and an iterative solution

The solution of Eq. (11) has been obtained by the iterative method of [12]. This is considered the reference solution, and is used as a standard for comparing the results by the three approximate methods.

The integral form of the resulting equation is evaluated by using a quadrature of the normal optical depth and by dividing the atmosphere up into layers of finite optical thickness. The integration over the zenith angle is accomplished by the trapezoidal rule, using a 2° discretization interval. This results in a system of linear algebraic equations, which is solved by the iterative procedure of Gauss-Seidel. The initial value of the source function is taken to include only primary scattering, and the iterative procedure is curtailed when successive iterative values differ by less than 0.001.

• Primary scattering approximation

The main burden computing the short wave flux divergence in a turbid atmosphere is in accounting for multiple scattering. Thus, a considerable reduction in computer time can be achieved by considering only primary scattering of the direct solar beam. In this case, the integral term of the source function [Eq. (5)] is eliminated, which yields the simplified expression

$$J(\tau; \mu, \phi) = \frac{F}{4} \exp - (\tau/\mu_0) P(\tau; \mu, \phi; -\mu_0, \phi_0).$$
 (19)

The primary scattering approximation is obtained by substituting Eq. (19) into Eq. (1). The solution of the resultant equation can be obtained analytically. However, for comparison purposes our calculations are based on discretizing the equation for optical thickness and azimuth angle, and solving the resulting system of linear equations by the Gauss-Seidel iterative technique. The validity of this approximation will be discussed below.

• No-scattering approximation

This approximation assumes absorption only by gases and aerosols. It is based on the hypothesis that the lack of irradiance of a given layer due to the neglect of scattering by the overlying atmosphere will be compensated for by a concomitant strengthening of the scatter-free solar beam reaching the layer. Herman and Yarger [22] have shown the method to be most realistic for a spectral region with strong gaseous absorption and small optical thickness, and the method has been used by various authors (e.g. [10]) for calculations of fluxes and heating rates.

In applying the no-scattering approximation, we let the scattering optical thickness and albedo of single scattering both vanish, and neglect the second term of the source function. Thus we have $\tau^{(s,r)} = \tau^{(s,m)} = \omega(\tau) = 0$, and the source function is that given in Eq. (19). The solution of the radiative transfer equation (1) then takes the form

$$I(\tau; \mu, \phi) = I(0; \mu, \phi) \exp \left[-(\tau^{(a,m)} + \tau^{(a)})/\mu \right].$$
 (20)

• Median wavelength approximation

In the strict sense, the equation of radiative transfer is valid only for monochromatic radiation; it may be used to compute radiation integrated over a wavelength interval, if band-averaged values for the scattering and absorption parameters are chosen. In the methods discussed above, this approach resulted in 80 unequal spectral bands. However, some investigators [5, 10] have suggested that even this is too computer time-consuming and have calculated flux values using radiation parameters evaluated at a single (median) wavelength. Radiation calculations applicable to this median wavelength, usually selected as about $0.5~\mu m$, are then assumed to be representative of the entire short wave spectrum.

To test this hypothesis, we have carried out two independent sets of calculations at two median wavelength values, $0.5150 \mu m$ and $0.725 \mu m$. The former value is close to that used by Atwater [10], while the latter selection is just beyond the portion of the spectrum where scattering by aerosols is at a maximum. This point is worth noting since the median wavelength approximation does take account of all orders of scattering. However, the transfer equation is evaluated only at the single wavelength value. These median wavelengths having been selected, 80 wavelength intervals throughout the entire solar spectrum were used to calculate the direct solar flux and azimuth-independent component of flux of diffuse skylight at the top of the radiation boundary layer. By using these quantities as input, the equation of radiative transfer is solved for the radiative boundary layer in a procedure parallel to that described for the reference method. However, the aerosol scattering and absorption parameters are taken to be those of the median wavelength. The gaseous transmission is evaluated by using the wavelength-independent formulation of Sasamori et al. [23]. Thus, the median wavelength approximation does consider both aerosol scattering and absorption and gaseous absorption of the direct and diffuse beams as they traverse the radiation boundary layer.

It is well established that the major gaseous absorber causing attenuation of the short wave radiation under normal atmospheric conditions is water vapor [24, 25]. Therefore, we consider only gaseous absorption by water vapor in the median wavelength approximation. Following Sasamori et al. [23], the attenuation of the direct solar

Table 1 Numerical methods for computing short wave flux divergence.

Computational method	Number of spectral bands	Gaseous absorption	Aerosol absorption	Order of scattering
Al median	1 (0.5150 μm)	water vapor	yes	multiple
A2 wavelength	$1(0.7250 \mu \text{m})$	water vapor	yes	multiple
B — no-scattering	80	water vapor, CO_2 , O_2 , O_3	yes	none
C — primary scattering	80	water vapor, CO_2 , O_2 , O_3	yes	primary
D — (reference)	80	water vapor, CO_2 , O_2 , O_3	yes	multiple

beam reaching the nth level can be written as

$$\tilde{T}_{wn} = \exp[-\tau_n^{(a)}/\mu_0]$$

= 1.0121 - 0.110(C_{wn} - 6.31 × 10⁻⁴)^{0.3}, (21)

where \bar{T}_{wn} is the wavelength transmission of water vapor and $C_{wn}(gm/cm^2)$ is the scaled water vapor amount above the *n*th level. For the absorption of the scattered beam as it passes through the *n*th layer, we follow the formulation given in Eq. (18) while using Eq. (21) for evaluating the transmission function.

Discussion of results

The qualitative characteristics of the methods outlined for solving the transfer equation are described in Table 1.

The ratios of the flux divergences resulting from Eqs. (18) and (21), as opposed to the detailed spectral method of Braslau and Dave [12], are shown in Fig. 2. The calculations are for levels within the radiation boundary layer. The results show significant deviations of the flux divergence ratio from unity, with a strong zenith angle dependency. The best agreement between the two methods is obtained for the long path length and large solar zenith angle of 80°. In this case, the ratio ranges from 0.86 to 1.07 at the top and bottom of the radiation boundary layer, respectively. The flux divergence ratios attain their worst values for a solar zenith of 0°, their ratios being 1.49 and 1.74 at the top and bottom of the radiation boundary layer, respectively. Except for long path lengths and large solar zenith angle, the wavelength-dependent method shows less absorption than does the wavelength-independent approach. It is obvious that Eq. (21) is not the optimally designed formulation for treating absorption due to water vapor. One could devote an entire independent study to obtaining a wavelength-independent transmission which might result in water vapor absorption approaching that obtained by using the reference method. This endeavor is beyond the scope of this paper. Equation (21) is used in conjunction with the median wavelength approximation solution to the transfer equation.

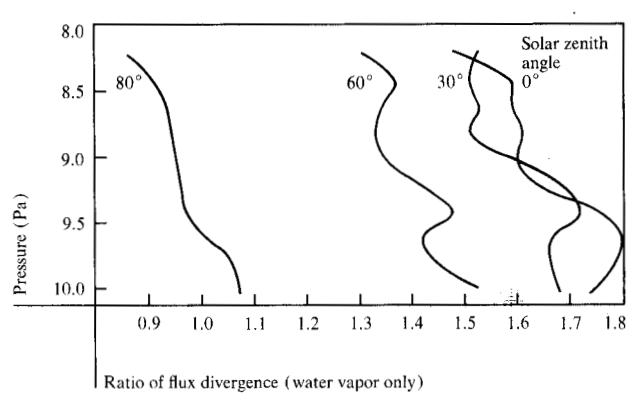
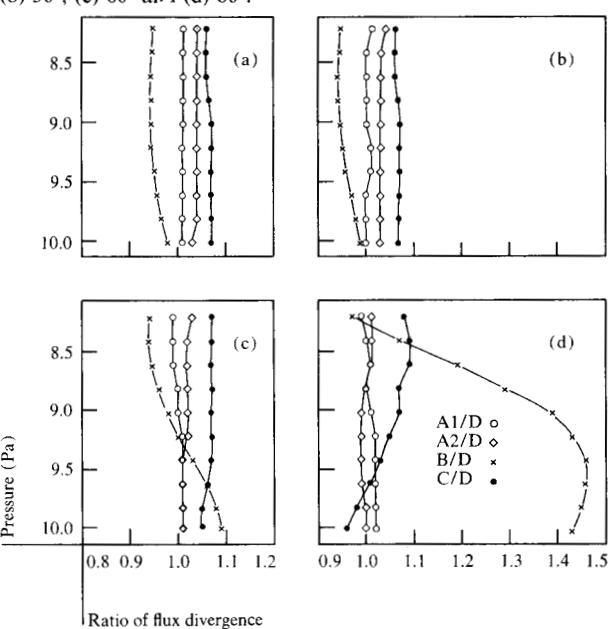


Figure 2 Vertical profile of the ratio of short wave flux divergence due to water vapor absorption using a wavelength-independent parameterization method compared to a wavelength-dependent method.

Figure 3 Vertical profile of the ratio of short wave flux divergence obtained by using approximate computational methods (A1, A2, B and C) compared to that obtained from the reference method (D). The results are for Haze L aerosol size distribution, a refractive index of 1.8-0.50 i, and solar zenith angles of (a) 0° , (b) 30° , (c) 60° and (d) 80° .



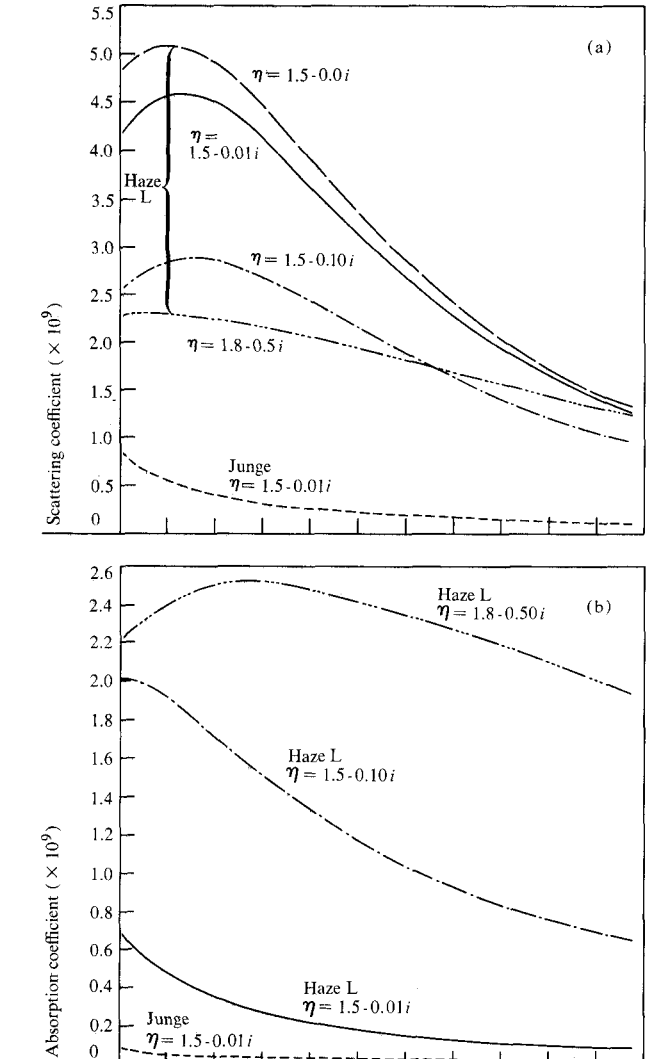


Figure 4 The scattering (a) and absorption (b) coefficient per average particle as a function of the wavelength for Haze L and Junge aerosol size distributions using different refractive indices.

1.5

0.3 0.5

0.7

Wavelength (µm)

The relative significance of absorption due to aerosols and gases in the radiation boundary layer has been calculated by Halpern and Coulson [26]. For the Haze L distribution the results were strongly solar zenith angle dependent. The total flux absorbed (in watts/cm²) in a 2-km column for a zenith angle of 0° varied from 0.389×10^{-2} , 1.348×10^{-2} , and 3.714×10^{-2} for refractive indices 1.5-0.0 i, 1.5-0.01 i, and 1.5-0.10 i, respectively. At 80° the absorption was 4.3×10^{-4} , 3.15×10^{-3} , and 9.78×10^{-9} , respectively. The flux absorbed by aerosols was an order of magnitude above that for gaseous absorption.

• Effect of various scattering approximations

For the sake of clarity and simplicity, we compute the ratio of flux divergence values obtained for each of the approximate methods to those for the reference method. The vertical profiles of this ratio in the radiation boundary layer are shown in Figs. 3 (a)-(d) for the four solar zenith angles $\theta_0 = 0^{\circ}$, 30°, 60° and 80°, respectively. The aerosol size distribution used is Haze L and the aerosol refractive index η is 1.80-0.05 i. For 0° , the median wavelength methods (A1 and A2), and the primary scattering method (C) result in flux divergence ratios greater than unity. Method C allows for over-absorption since it is an incomplete solution to Eq. (1). For methods A1 and A2 the excessive absorption of flux is a consequence of the fact that both the direct and diffuse fluxes incident at the top of the boundary layer are integrated over wavelength. whereas the flux divergence within the radiation boundary layer is computed by the use of values of aerosol scattering and absorption coefficients per average particle evaluated at a specific wavelength. In Figs. 4(a) and 4(b), we present the wavelength dependency of these quantities. The values at wavelengths $\lambda = 0.5150$ and $0.7250 \mu \text{m}$ for $\eta = 1.80 - 0.50 i$ are close to the maximum for the entire solar spectrum considered. The slightly larger flux divergence ratio for method A2 (λ = $0.7250 \mu m$) is related to the small decrease in the normal scattering and absorption optical thickness for this wavelength compared to that used for method A1 (λ = $0.5150 \mu m$).

The no-scattering approximation method (B) shown in Fig. 3 results in a flux divergence ratio less than unity throughout the radiation boundary layer for $\theta_0 = 0^{\circ}$ and 30°. The omission of scattering in the direct solar beam causes greater flux to reach all levels in the radiation boundary layer. Also, the downward diffuse flux that is incident on the top of the layer undergoes only absorption as it penetrates into this layer. Therefore, its magnitude is less than it would have been had multiple scattering from the direct beam been present. The ratio for the flux divergence values calculated by method B should be unity, provided the increase in the magnitude of the direct beam flux is compensated by the lack of the upward diffuse flux and a reduced downward diffuse flux. The results at θ_0 = 0° indicate that such a balance does not occur. This is due in part to the large scattering coefficient per average particle of the aerosol chosen for these computations [Fig. 4(a)]. Thus the enhanced direct beam flux overcompensates for the reduced diffuse beam flux. This causes a reduction in the flux divergence, and explains why the values for these ratios are less than unity.

In general, flux divergence ratios shown in Fig. 3, $\theta_0 = 30^{\circ}$ and 60°, show similar trends for all methods except for method B and $\theta = 60^{\circ}$. Here, the ratio changes from less than unity to greater than unity at levels below 923 mb

(9.23 Pa). At $\theta_0 = 80^\circ$, the ratio takes on large positive values at all but the top part of the radiation boundary layer. Longer path lengths of $\theta_0 = 60^\circ$ and 80° enhance the importance of aerosol scattering. At large solar zenith angles the downward diffuse beam becomes the dominating component for flux divergence. The neglect of aerosol scattering causes a substantial decrease of the diffuse component, so the scattering approximation of method B leads to the indication of excessive absorption shown for $\theta_0 = 80^\circ$ in Fig. 3.

• Effect of aerosol refractive index upon the noscattering approximation

The sensitivity of the reference method to changes in η was investigated by Halpern and Coulson [26] and was discussed earlier. To establish the sensitivity of the various approximation methods, we first present the ratio of the flux divergence of method B to the reference method for η values of 1.5-0.00 i, -0.01 i, and -0.10 i with aerosol model Haze L. The ratios of the four zenith angles are shown in Fig. 5. The flux divergences are all less than unity when $\theta_0 = 0^{\circ}$. This is consistent with the results presented in Fig. 3 for $\eta = 1.80 - 0.5 i$, but the ratios are all smaller in magnitude than those in Fig. 3. In Fig. 5 the noscattering approximation is closest to the reference method (i.e. the ratio is closest to unity) for $\eta = 1.50 - 0.1 i$. For $\theta_0 = 30^\circ$, the ratios are somewhat smaller than those at 0°, whereas for $\theta_0 = 60^{\circ}$ and 80°, they are significantly larger. At these larger angles, aerosols with $\eta = 1.50$ -0.0 i and -0.01 i have almost identical flux divergence ratios, and ratios for the three refractive indices have values which are greater than unity at levels below 943 mb (9.43 Pa). Very large ratios are found for all three η values at $\theta = 80^{\circ}$, as they were for strongly absorbing aerosols ($\eta = 1.80$ -0.5 i) in Fig. 3. Thus, comparison of the data indicates that an increase in aerosol absorption makes the no-scattering approximation agree more closely with the reference method.

The reason for the divergence ratios having values which are less than unity at $\theta_0 = 0^{\circ}$ and 30° has previously been explained. The results of Fig. 5 show that for small solar zenith angles, the no-scattering approximation is best for highly absorbing and nonabsorbing aerosols, with larger errors for the case of moderate absorption. This apparent inconsistency can be explained by referring to the scattering and absorption coefficient per average particle for these aerosols in Figs. 4(a) and 4(b). For the nonabsorbing aerosol ($\eta = 1.50-0.0 i$), the no-scattering approximation correctly accounts for absorption of the direct beam by gases, but the lack of scattering results in no diffuse component. The lack of absorption of this diffuse radiation causes the no-scattering approximation to give a ratio (shown in Fig. 5) of less than unity at the smaller solar zenith angles. The relatively poor approximation at-

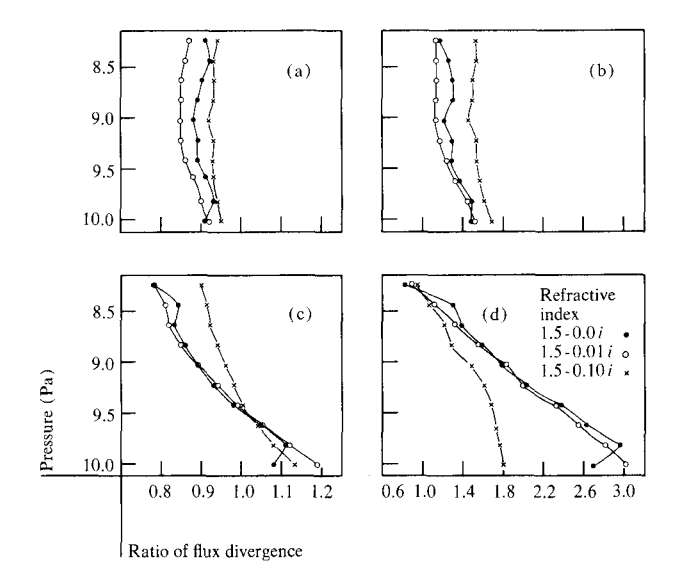


Figure 5 Vertical profile of the ratio of the short wave flux divergence obtained by using the no-scattering approximation method (B) compared to that obtained by using the reference method (D) for aerosols of three different refractive indices: (\bullet) 1.5-0.0 i, (\circ) 1.5-0.1 i, and (\times) 1.5-0.10 i. The results are for Haze L aerosol size distribution and solar zenith angles of (a) 0 $^{\circ}$, (b) 30 $^{\circ}$, (c) 60 $^{\circ}$ and (d) 80 $^{\circ}$.

tained by the no-scattering approximation for the case of moderate aerosol absorption ($\eta=1.50\text{-}0.01~i$) is caused by significant absorption by gases and aerosols in the approximation, but with little diminution of scattering in the reference method. Thus the ratio of flux divergence for the two methods is less for this case than for that of smaller index of refraction. The approximation is again improved for the large imaginary index of refraction (0.1 i) for small angles. This occurs because of strong absorption of the scattered radiation in the reference method without a commensurate increase in absorption of the direct beam for the no-scattering approximation for the case of small solar zenith angles.

For the solar zenith angles of 60° and 80°, the flux divergence ratio of Fig. 5 becomes significantly larger than unity in the lower portion of the radiation boundary layer. At these angles, the lower path length and consequent larger scattering optical thickness cause enhancement of the downward diffuse flux at the expense of the direct beam. The decrease of the direct plus diffuse beam is caused by some added backscattering. The reference method takes into account the backscattered radiation, whereas the no-scattering approximation does not. Consequently, in the reference method, there is less energy available for absorption. This causes the flux divergence ratio to be greater than unity and the effect increases with increasing zenith angle.

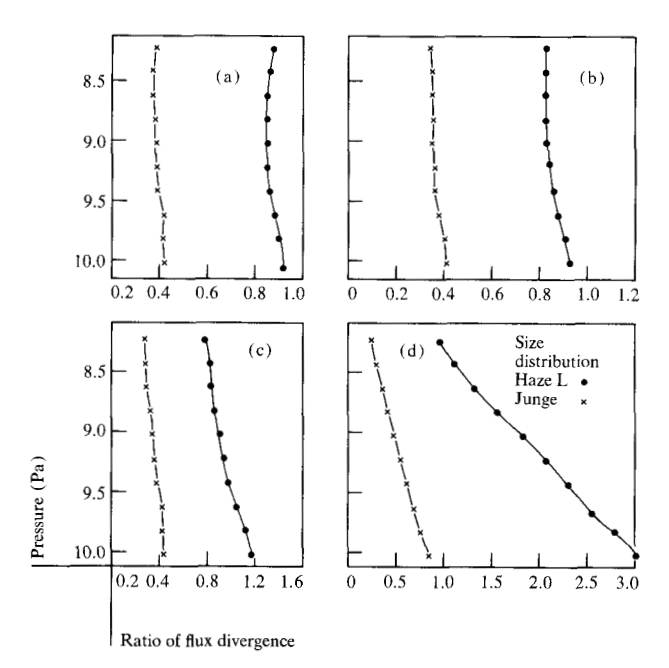
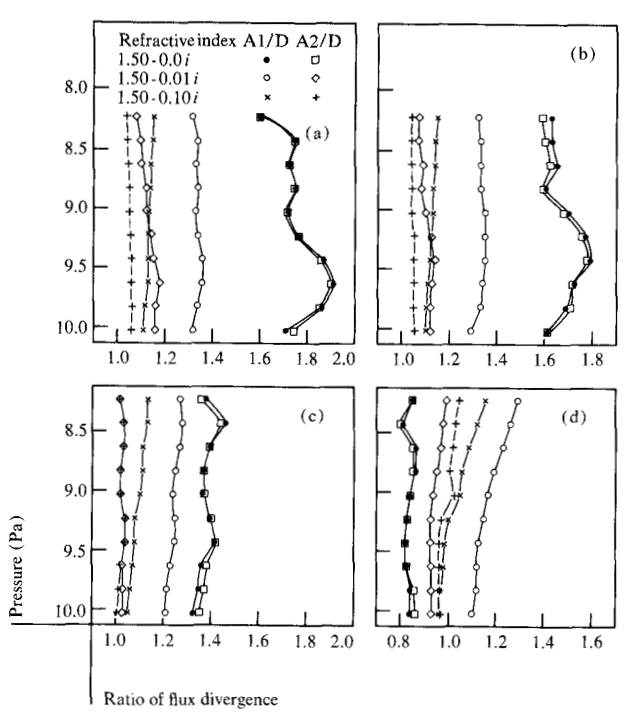


Figure 6 Vertical profile of the ratio of the short wave flux divergence obtained by using the no-scattering approximation method (B) compared to that obtained by using the reference method (D) for Haze L (\bullet) and Junge (\times) aerosol size distributions. Results are for a refractive index of 1.50-0.01 *i* and solar zenith angles of (a) 0°, (b) 30°, (c) 60° and (d) 80°.

Figure 7 Vertical profile of the ratio of the short wave flux divergence obtained by using the median wavelength approximation methods (A1 and A2) compared to that obtained by using the reference method (D) for aerosols of three different refractive indices. The results are for the Haze L aerosol size distribution and solar zenith angles of (a) 0°, (b) 30°, (c) 60° and (d) 80°.



Effect of aerosol size distribution upon the noscattering approximation

A comparison of flux divergence ratios for Haze L and Junge aerosol distributions for an index of refraction of η = 1.50-0.01 i is shown for four solar zenith angles in Fig. 6. The no-scattering approximation gives better results for the Haze L model than for the Junge distribution for all $\theta_0 \le 60^\circ$. This is a consequence of the much greater role that scattering plays in the extinction of radiation by the individual particles of the Junge size distribution in combination with the larger total number of Junge particles necessary for equal mass for the two distributions. The many very small particles for the Junge case are particularly important for light scattering. For instance, the ratio of scattering to absorption coefficients is 13 for Junge particles but only 10 for the particles of Haze L for method B. Thus the neglect of scattering causes larger errors for the Junge distribution than for Haze L. For large solar zenith angles, both models produce strong scattering, thereby rendering the no-scattering approximation an inaccurate representation of reality.

• Effect of aerosol refractive index upon the median wavelength approximation

The ratio of flux divergence computed by the median wavelength approximation to that computed by the reference method for the Haze L particle distribution is shown for two different median wavelengths ($\lambda = 0.7250 \mu m$ for method A2, and $\lambda = 0.5150 \mu m$ for method A1) and various combinations of refractive indices and solar zenith angles in Fig. 7. This approximation gives too large a flux divergence at all solar zenith angles except $\theta_0 = 80^{\circ}$, in which case scattering effects in the long atmospheric path lengths traversed by the radiation are important at all wavelengths as determined by the reference method. For smaller solar zenith angles, the large scattering and absorption coefficients [see Figs. 4(a) and 4(b)] that exist at wavelengths 0.5150 and 0.7250 µm make the flux divergence very strong for the median wavelength approximations based on those particular wavelengths. With a nonabsorbing aerosol ($\eta = 1.50-0.0 i$), the approximation gives about the same divergence for the two wavelengths, a result expected from the upper curve of Fig. 4(a). As the absorption becomes significant, however, the flux divergence becomes less for $\lambda = 0.7250 \,\mu\text{m}$ than for $\lambda =$ $0.5150 \mu m$. The difference is strongest for $\eta = 1.50 - 0.0 i$, a result that is consistent with the absorption coefficient curves of Fig. 4(b). For larger amounts of absorption ($\eta =$ 1.50-0.10 i), the median wavelength approximation gives the more realistic results, particularly for the longer of the two wavelengths, as would be anticipated from the fact that the aerosol scattering and absorption coefficients are lower for $\lambda = 0.7250 \,\mu\text{m}$ than for $\lambda = 0.5150 \,\mu\text{m}$ (Fig. 4).

The ratio of the flux divergence for methods A1 and A2 in the case of the nonabsorbing aerosol are of the same magnitude as those presented in Fig. 7 for gaseous absorption. In particular the same zenith angle dependence is present in both figures. Therefore the method of treating gaseous absorption is critical for flux divergence calculations in the presence of such an aerosol. However, for the absorbing aerosols, the flux divergence ratios show marked improvement. While this might appear to be the result of compensating errors, the magnitude of the absorption caused by these aerosols was shown to be far in excess of the absorption by gases. Using the reference method, the ratios of absorbed flux for a nonabsorbing aerosol ($\eta = 1.50-0.0 i$) to that for a moderate-absorbing aerosol ($\eta = 1.50-0.01 i$) at 0° and 80° are 3.5 and 7.3, respectively. For the strong-absorbing aerosol, ($\eta = 1.5$ -0.10 i), these ratios are 9.5 and 22.7 at 0° and 80° , respectively. Therefore, the effect of the absorption by aerosols completely masks that due to gases. The results of the median wavelength approximations are a function of the absorbing quality of the aerosol.

Effect of aerosol size distribution upon the median wavelength approximation

The aerosol size distribution has a very strong effect on the results obtained with the median wavelength approximation, as shown in Fig. 8 for a moderately absorbing aerosol ($\eta = 1.50-0.01 i$). The flux divergence is much too low at both $\lambda = 0.5150$ and 0.7250 μ m for the Junge distribution, whereas it is generally too high for the Haze L model. This discrepancy can be explained by the greatly different scattering and absorption coefficients for the two distributions shown in Fig. 4. The much smaller values of these coefficients for the Junge distribution, in combination with the fact that computations by the reference method were for the Haze L distribution, yields the small ratios shown by the curves. The scattering and absorption coefficients are slightly higher at $\lambda = 0.5150 \,\mu\text{m}$ than for λ = $0.7250 \mu m$, resulting in correspondingly higher ratios of flux divergence for the shorter wavelength for both distributions.

Effect of aerosol refractive index upon the primary scattering approximation

In this approximation, primary scattering of the direct solar beam is taken into account, but all higher orders of scattering are neglected. The lack of a complete solution of the transfer equation causes unrealistically high values of flux divergence, as shown in Fig. 9. For a nonabsorbing aerosol ($\eta = 1.50\text{-}0.0 i$), the flux divergence computed by the primary scattering approximation is 6 to 20 times greater than that computed by the reference method. Introduction of aerosol absorption ($\eta = 1.50\text{-}0.01 i$ and -0.10 i) improves the approximation considerably, but the pri-

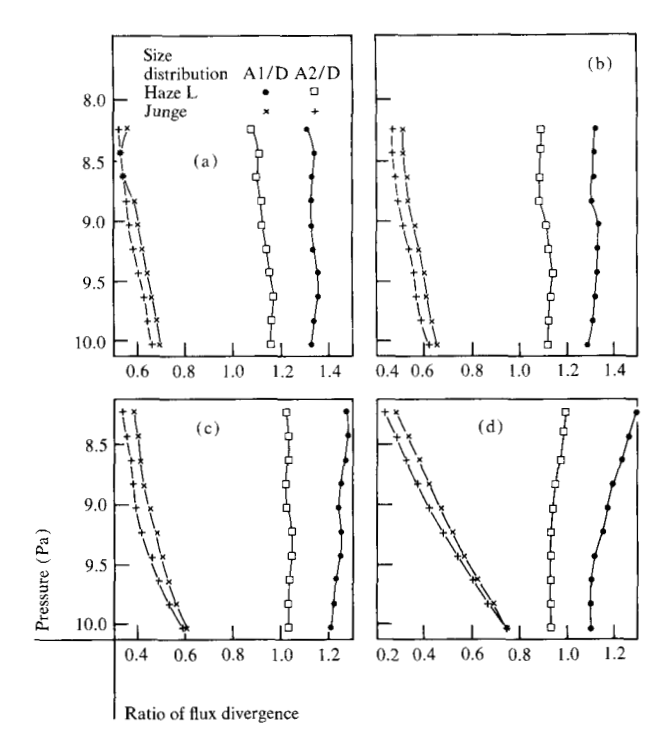
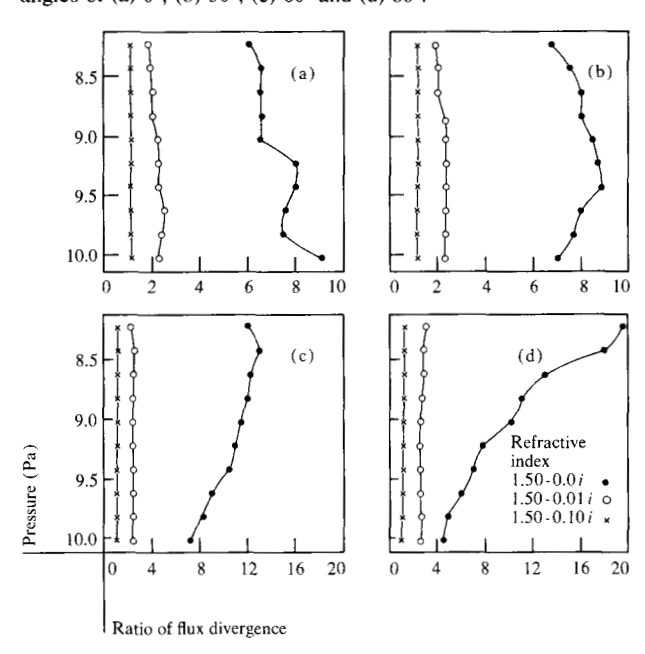


Figure 8 Vertical profile of the ratio of the short wave flux divergence obtained by using the median wavelength approximation methods (A1 and A2) compared to that obtained by using the reference method (D) for Haze L and Junge aerosol size distributions. The results are for the refractive index $\eta = 1.5 \cdot 0.01 i$ and solar zenith angles of (a) 0° , (b) 30° , (c) 60° and (d) 80° .

Figure 9 Vertical profile of the ratio of the short wave flux divergence obtained by using the primary scattering approximation method (C) compared to that obtained by using the reference method (D) for three different aerosol refractive indices. The results are for Haze L aerosol size distribution and solar zenith angles of (a) 0° , (b) 30° , (c) 60° and (d) 80° .



mary scattering approximation yields results similar to those for the reference method only for strong absorption accompanied by large optical path lengths ($\theta = 60^{\circ}$ and 80°).

The absorption coefficients used in both methods are identical. However, the over-absorption in the primary scattering approximation results from the incomplete solution to the equation of transfer. The neglecting of the higher orders of scattering causes a decrease in both the downward diffuse and upward diffuse beams. The loss in flux increases rapidly with increase in the scattering optical thickness. The presence of an increasingly absorbing aerosol causes absorption of some of the flux that would be otherwise unaccounted for. This causes the reduced ratios for these aerosols shown in Fig. 9. The over-absorption will decrease, approaching that of the reference method as increasingly higher orders of scattering are included. As can be seen from the data of Fig. 9, absorption by aerosol particles decreases the effects of overabsorption, but this approximation must be viewed as of marginal value in practical applications.

Conclusions

From the flux divergence results presented in this study. it appears that the no-scattering approximation and the median wavelength approximation are superior to the primary scattering approximation for evaluating short wave flux divergence in the presence of aerosols. When choosing between these methods one must carefully consider the computational time required. The time necessary for calculating the flux divergence for twenty levels in the radiation boundary layer for four solar zenith angles varies over two orders of magnitude for the various methods. The relative times were: reference method (D), 1.0, primary scattering approximation method (C), 0.1, no-scattering approximation method (B), 0.01, and median wavelength approximation methods (A1 and A2), 0.02. The twofold decrease in computational time for method B over methods A1 or A2 makes the former scheme quite attractive. However, from the point of view of overall accuracy, it appears that all of the approximation methods may be considerably inaccurate in some circumstances and accurate in others. Therefore, care should be exercised when using only one of these approximations.

If it is important to treat the scattering effects of aerosols (in the evaluation of upward and downward diffuse fluxes or intensities), the scattering should be calculated by using the reference method. Alternately, a modified version of the median wavelength approximation method might be used, where the transfer equation is evaluated at multiple wavelengths, rather than at a single wavelength. In this case, the absorption and scattering coefficients per average particle, as well as the gaseous absorption coefficients, could be determined for six to ten wide spectral

bands. This approach would increase the computational time requirements, but would allow for the incorporation of aerosol radiation parameters that are more representative of the total solar spectrum. In addition, the problem of a wavelength-independent parameterization of gaseous absorption would be alleviated.

Acknowledgment

The authors thank J. V. Dave of the IBM Palo Alto Scientific Center for his guidance and generous assistance during this investigation.

References

- K. Ya. Kondratyev, O. B. Vasilyev, V. S. Grishenhkin, M. A. Prokofyev, L. S. Chapursky, and L. S. Ivlev, "Spectral Radiative Flux Divergence in the Troposphere," Proceedings of the International Radiation Symposium (Radiation Commission of the International Association of Meteorology and Physics, H. J. Bolle, Meteorological Institute of the University of Munich, West Germany), Sendai, Japan (1973).
- D. W. Reynolds, T. H. Van der Haar, and S. K. Cox, "The Effect of Solar Radiation Absorption in the Tropical Troposphere," J. Appl. Meteorol. 14, 433 (1974).
- S. I. Rasool and S. N. Schneider, "Atmospheric Carbon Dioxide and Aerosol Effects of Large Increases in Global Climate," *Science* 173, 138 (1971).
- 4. J. M. Mitchell, Jr., "The Effect of Atmospheric Aerosols on Climate with Special Reference to Temperature Near the Earth's Surface," J. Appl. Meteorol. 10, 703 (1961).
- A. A. Lacis and J. E. Hansen, "A Parameterization for the Absorption of Solar Radiation in the Earth's Atmosphere," J. Atmos. Sci. 31, 118 (1974).
- I. F. Hand, "Transmission of the Total and Infrared Component of Solar Radiation Through a Smoky Atmosphere," Bull. Amer. Meteorol. Soc. 24, 201 (1943).
- A. R. Meethan, "Atmospheric Pollution in Leichester," DSIR Tech. Paper No. 1, H. M. Stationery Office, London, England (1945).
- 8. J. L. Montheith, "Local Differences in the Attenuation of Solar Radiation over Britain," Q. J. Roy. Meteorol. Soc. 92, 254 (1966).
- 9. J. T. Peterson and E. C. Flowers, "Urban-Rural Solar Radiation and Aerosol Measurements in St. Louis and Los Angeles," *Preprint Symposium on Atmospheric Diffusion and Air Pollution*, (American Meteorological Society, Boston, MA), Santa Barbara, CA, 1974, p. 129.
- M. A. Atwater, "Radiative Effects of Pollutants on the Atmospheric Boundary Layer," J. Atmos. Sci. 28, 1367 (1971).
- R. W. Bergstrom, Jr. and R. Viskanta, "Modeling of the Effects of Gaseous and Particulate Pollutants in the Urban Atmosphere. Part I: Thermal Structure," J. Appl. Meteorol. 12, 901 (1973).
- 12. N. Braslau and J. V. Dave, "Effect of Aerosols on the Transfer of Solar Energy Through Realistic Model Atmospheres. Part I: Non-absorbing Aerosols," *J. Appl. Meteorol.* 12, 601 (1973).
- 13. J. V. Dave and J. Gazdag, "A Modified Fourier Transform Method for Multiple Scattering Calculations in a Plane Parallel Atmosphere," *Appl. Opt.* **9**, 1457 (1970).
- J. V. Dave, "Coefficients of the Legendre and Fourier Series for the Scattering Functions of Spherical Particles," Appl. Opt. 9, 2673 (1970).
- B. M. Herman and S. R. Browning, "The Effect of Aerosols on the Earth-Atmosphere Albedo," J. Atmos. Sci. 32, 1430 (1975).
- J. Cartwright, G. Nagelschmidt, and J. W. Skidmore, "Study of Air Pollution with the Electron Microscope," Q. J. Roy. Meteorol. Soc. 82, 82 (1956).

- 17. J. T. Twitty and J. A. Weinman, "Radiative Properties of Carbonaceous Aerosols," J. Appl. Meteorol. 10, 725 (1971).
- 18. C. E. Junge, "The Size Distribution and Aging of Natural Aerosols as Determined from Electrical and Optical Data on the Atmosphere," *J. Meteorol.* 12, 13 (1955).
- 19. D. Deirmendjian, Electromagnetic Scattering on Spherical Polydispersions, American Elsevier Publishing Co., New York, 1969.
- J. J. DeLuisi, I. H. Blifford, Jr., and J. A. Takamine, "Models of Tropospheric Aerosol Size Distribution Derived from Measurements at Three Locations," J. Geophys. Res. 77, 4529 (1972)
- R. A. McClatchey, R. W. Fenn, J. E. A. Selby, J. S. Garing, and F. E. Volz, "Optical Properties of the Atmosphere," AFCRL Report 70-0527; Environ. Res. Papers, No. 331; Air Force Cambridge Research Laboratories, Cambridge, MA, 1970.
- 22. B. M. Herman and D. N. Yarger, "The Effect of Absorption on a Rayleigh Atmosphere," J. Atmos. Sci. 22, 644 (1965).
- 23. T. Sasamori, J. London, and D. V. Hoyt, "Radiation Budget of the Southern Hemisphere," *Meteorol. Monogr.* 13, 9 (1972)

- W. T. Roach, "The Absorption of Solar Radiation by Water Vapor and CO₂ in a Cloudless Atmosphere," Q. J. Roy. Meteorol. Soc. 31, 364 (1961).
- D. E. Burch, D. A. Gryvnak, E. B. Singelton, W. F. France, and D. Williams, "Infrared Absorption by Carbon Dioxide, Water Vapor, and Minor Atmospheric Constituents," AFCRL Report AF19(604)-2633, Air Force Cambridge Research Laboratories, Cambridge, MA, 1962.
- 26. P. Halpern and K. L. Coulson, "A Theoretical Investigation of the Effect of Aerosol Pollutants on Shortwave Flux Divergence in the Lower Troposphere," J. Appl. Meteorol. 15, 464 (1976).

Received August 17, 1977; revised November 22, 1977

P. Halpern is located at the IBM Palo Alto Scientific Center, P.O. Box 10500, Palo Alto, California 94304; K. L. Coulson is located at the University of California, Davis, California 95616.